Received: 9 April 2019 | Revised: 30 May 2019 | Accepted: 5 July 2019

DOI: 10.4218/etrij.2019-0176

ORIGINAL ARTICLE

ETRI Journal WILEY

Efficient cell design and fabrication of concentration-gradient composite electrodes for high-power and high-energy-density all-solid-state batteries

Ju Young Kim | **Jumi Kim** | **Seok Hun Kang** | **Dong Ok Shin** | **Myeong Ju Lee** | **Jimin Oh** | **Young-Gi Lee** | **Kwang Man Kim**

ICT Creativity Research Laboratory, Electronics and Telecommunications Research Institute, Daejeon, Rep. of Korea

Correspondence
Ju Young Kim and Kwang Man Kim, ICT Creativity Research Laboratory, Electronics and Telecommunications Research Institute, Daejeon, Rep. of Korea.
Email: juyoung@etri.re.kr; kwang@etri.re.kr

Funding information
This work was supported by the Technology Development Program to Solve Climate Changes of the National Research Foundation (NRF) funded by the Ministry of Science & ICT (2017M1A2A2044492) and the R&D Convergence Program (14-02-KITECH) of the National Research Council of Science and Technology (NST) of Korea.

All-solid-state batteries are promising energy storage devices in which high-energy-density and superior safety can be obtained by efficient cell design and the use of nonflammable solid electrolytes, respectively. This paper presents a systematic study of experimental factors that affect the electrochemical performance of all-solid-state batteries. The morphological changes in composite electrodes fabricated using different mixing speeds are carefully observed, and the corresponding electrochemical performances are evaluated in symmetric cell and half-cell configurations. We also investigate the effect of the composite electrode thickness at different charge/discharge rates for the realization of all-solid-state batteries with high-energy-density. The results of this investigation confirm a consistent relationship between the cell capacity and the ionic resistance within the composite electrodes. Finally, a concentration-gradient composite electrode design is presented for enhanced power density in thick composite electrodes; it provides a promising route to improving the cell performance simply by composite electrode design.

KEYWORDS
all-solid-state batteries, composite electrode, concentration gradient, energy storage devices, solid electrolytes

1 | INTRODUCTION

All-solid-state batteries with a bipolar stacked configuration are promising next-generation secondary batteries owing to their high-energy-density [1–4]. In contrast to liquid electrolytes in conventional lithium-ion batteries, the solid electrolytes in all-solid-state batteries make it possible to design a highly compact cell, which enables reduction of the volumetric cell capacity [5–7]. To achieve this, it is essential to develop solid electrolytes with electrochemical properties comparable to those of liquid electrolytes. To this end, researchers have performed intensive studies that have produced various solid electrolytes, such as inorganic oxide or sulfide solid electrolytes, organic polymeric electrolytes, and gel electrolytes [8–11]. In addition, an important issue in fabricating all-solid-state batteries with superior performance is the effective design of the composite electrode, and specifically of the spatial arrangement of individual composite components. In conventional lithium-ion batteries with liquid electrolytes, liquid electrolyte flow enables the formation of

Ju Young Kim and Jumi Kim contributed equally to this work.

a continuous ionic pathway within the electrodes and conformal contact with the active materials in the electrodes, resulting in facile transport of lithium ions within the electrodes and low charge transfer resistance between the active materials and the liquid electrolyte. However, these advantages are absent when solid electrolytes are used.

To obtain a continuous ionic pathway and conformal contact, the solid-state electrodes need to include solid electrolytes as well as active materials [12]. Therefore, the fabrication method of the composite electrode becomes a crucial concern [13]. For example, the mixing processes are closely related to the distribution of each electrode component, and the cell specifications, such as the compositions of the solid electrolyte and active material and the thickness of the composite electrodes, can significantly affect the cell performance. To address these issues, various approaches have been suggested, for example, direct coating of solid electrolytes on active materials and infiltration of solid electrolytes within prefabricated electrodes [6,10,14–17].

Here we present a systematic study of the formation of composite electrodes with reasonable performance using electrochemical impedance measurement and morphological observation. The study confirms that the cell performance depends strongly on the mixing conditions of the electrode and that a mild mixing process is desirable. In addition, we studied the dependence of the cell performance on the electrode thickness, which is strongly related to the ion transport within the composite electrodes. On the basis of the results, we propose concentration-gradient composite electrodes. A composite configuration with a high concentration of the solid electrolyte near the solid electrolyte layer sandwiched between the anode and the cathode enables facile ion transport to the active materials within the composite electrodes, improving the cell rate performance.

2 | EXPERIMENTAL SECTION

2.1 | Fabrication of all-solid-state batteries

All syntheses were conducted in an argon-filled glove box (MBraun). Li_2S–P_2S_5 glass ceramics (LPS) was prepared by conventional mechanical milling and subsequent heat treatment [18]. For mechanical milling of stoichiometric amounts of the Li_2S (Sigma-Aldrich, 99.98%) and P_2S_5 (Sigma-Aldrich. 99%) precursors, a planetary ball mill (Pulverisette 7PL, Fritsch GmbH) was used with 5 mm zirconia balls. The rotation speed was 800 rpm, and the mixing time was 10 hours. The resulting mixture was heat-treated at 270 °C for 2 hours. To obtain composite electrodes, the active material and solid electrode were mixed at various weight ratios using a Thinky mixer with 5 mm zirconia balls for 20 minutes. The composite anode was demonstrated using natural graphite (NG). To fabricate an all-solid-state anode half-cell, composite powders were spread on pre-pelletized LPS (150 mg) and pelletized by mechanical pressing (over 300 MPa) [19]. The amount of composite powder determined the loading level of the active material and the thickness of the composite electrode. The thickness of the composite electrode was measured by a conventional micrometer caliper. Lithium metal (300 μm thickness, Honjo Metal Co.) was attached to the other surface of the pre-pelletized LPS. To obtain a concentration-gradient composite electrode, repeated processes of spreading and pelletization of the composite powders with different blending ratios were performed. A concentration-gradient composite electrode with a three-layered composite structure was designed, and the composite electrodes were fabricated at a thickness of ~33 μm regardless of the blending ratio.

2.2 | Characterization

Scanning electron microscopy (SEM, Hitachi S-4800) and energy-dispersive X-ray spectroscopy (EDS, Bruker XFlash 6i100) were used for morphological observation and elemental mapping, respectively. The ionic conductivity was determined from complex impedance spectra measured using a frequency response analyzer (Solartron HF 1225 Gain-Phase Analyzer) in a frequency range of 10^{-1} to 10^5 Hz at room temperature. The electrochemical performance of the all-solid-state batteries was investigated using a cycle tester (Toyo Systems) at 60 °C.

3 | RESULTS AND DISCUSSION

To determine the ionic transport properties of the composite electrodes, composite symmetric cells were used (Figure 1A). In a full-cell configuration with different anodes and cathodes, the impedance can be measured, but in this case, the reaction complexity of individual electrodes generally makes precise analysis difficult [20,21]. To circumvent this issue, symmetric cells with identical electrodes at each end of the solid electrolyte layer can be used. Thus, we fabricated a composite symmetric cell consisting of NG and LPS to evaluate the ionic transport within the composite electrodes.

According to the transmission line model (TLM) without Faradaic reactions, the impedance of the composite electrode in the composite symmetric cell, $Z_{\text{composite}}$, is given by [20–22]

$$Z_{\text{composite}} = R_{\text{electrolyte}} + \sqrt{\frac{R_{\text{ion}}}{i\omega C_{\text{dl}}}} \coth \sqrt{R_{\text{ion}} i\omega C_{\text{dl}}}, \quad (1)$$

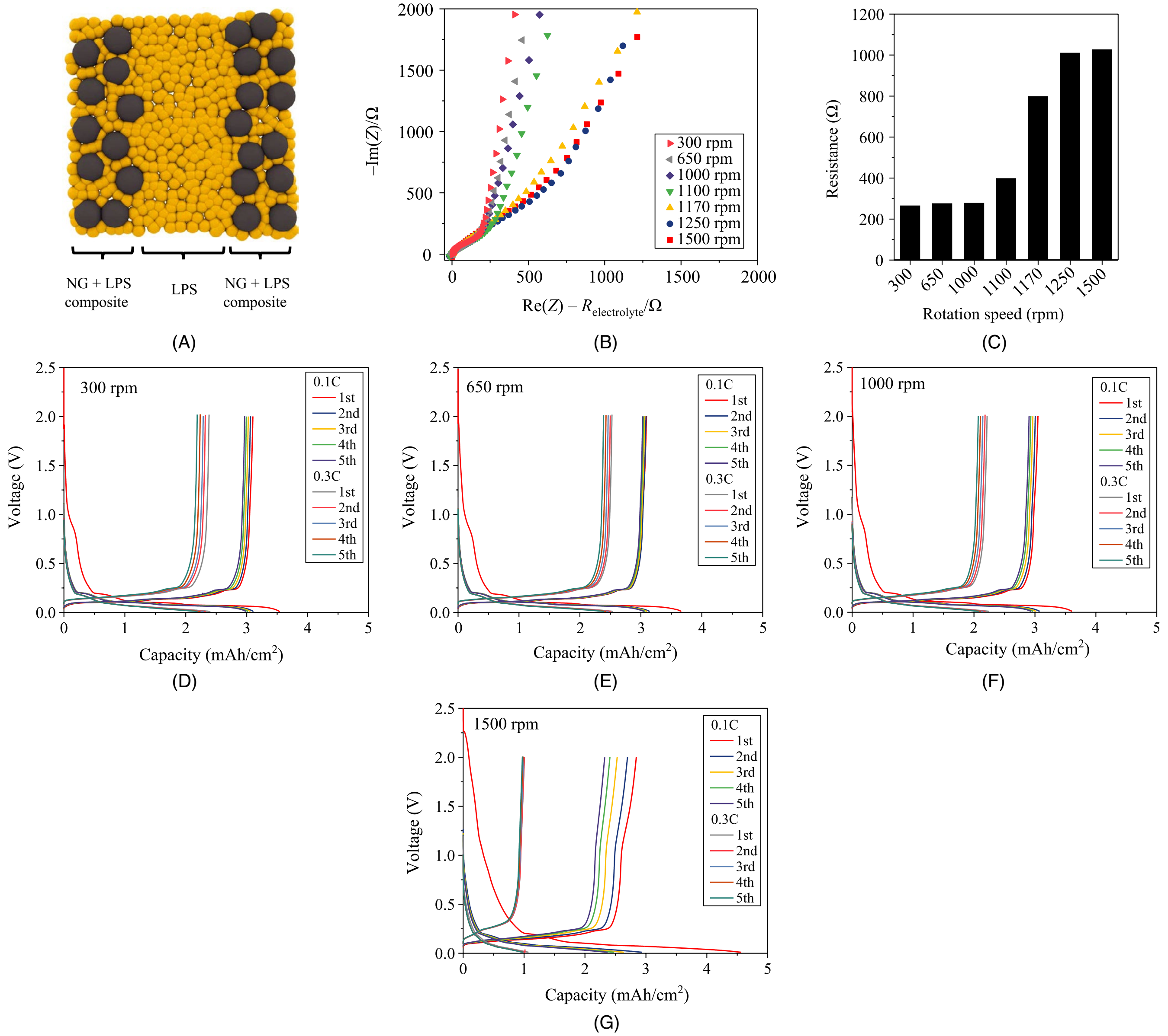

FIGURE 1 (A) Schematic illustration of composite symmetric cell, (B) impedance results of composite electrodes for various mixing conditions, and (C) corresponding resistance calculated from TLM analysis. (D–G) charge/discharge profiles of composite electrodes

where ω is the angular frequency, $R_{\text{electrolyte}}$ is the bulk ion transport resistance of the middle solid electrolyte layer, R_{ion} is the total ion transport resistance within the composite electrodes, and C_{dl} is the total double-layer capacitance at the interface between the active material and the solid electrolyte. The capacitances can be replaced by constant phase elements. The total ion transport resistance can be extracted from the real part of the impedance in the low-frequency regime as follows:

$$Z'_{\omega \to 0} = R_{\text{electrolyte}} = \frac{1}{3} R_{\text{ion}}. \tag{2}$$

By using this approximation of the impedance results, the ion transport properties of the composite electrodes can be obtained by measuring the impedance of the symmetric cells. Seven samples with NG as the active material (60 wt%) and LPS as the solid electrolyte (40 wt%) were prepared under different mixing conditions (300, 650, 1000, 1100, 1170, 1250, and 1500 rpm), and the ion transport properties were tested in the symmetric configuration. The loading level of each composite electrode was controlled at 15.2 mg/cm^2, and the corresponding composite thickness was ~63 μm. As shown in Figure 1B, these samples did not show any charge transfer reaction, so the approximation without Faradaic reactions can be used to describe our composite electrode [21]. The three samples with mixing conditions of 300, 650, and 1000 rpm exhibited similar profiles, but the other samples were different. Using the TLM approximation, we calculated

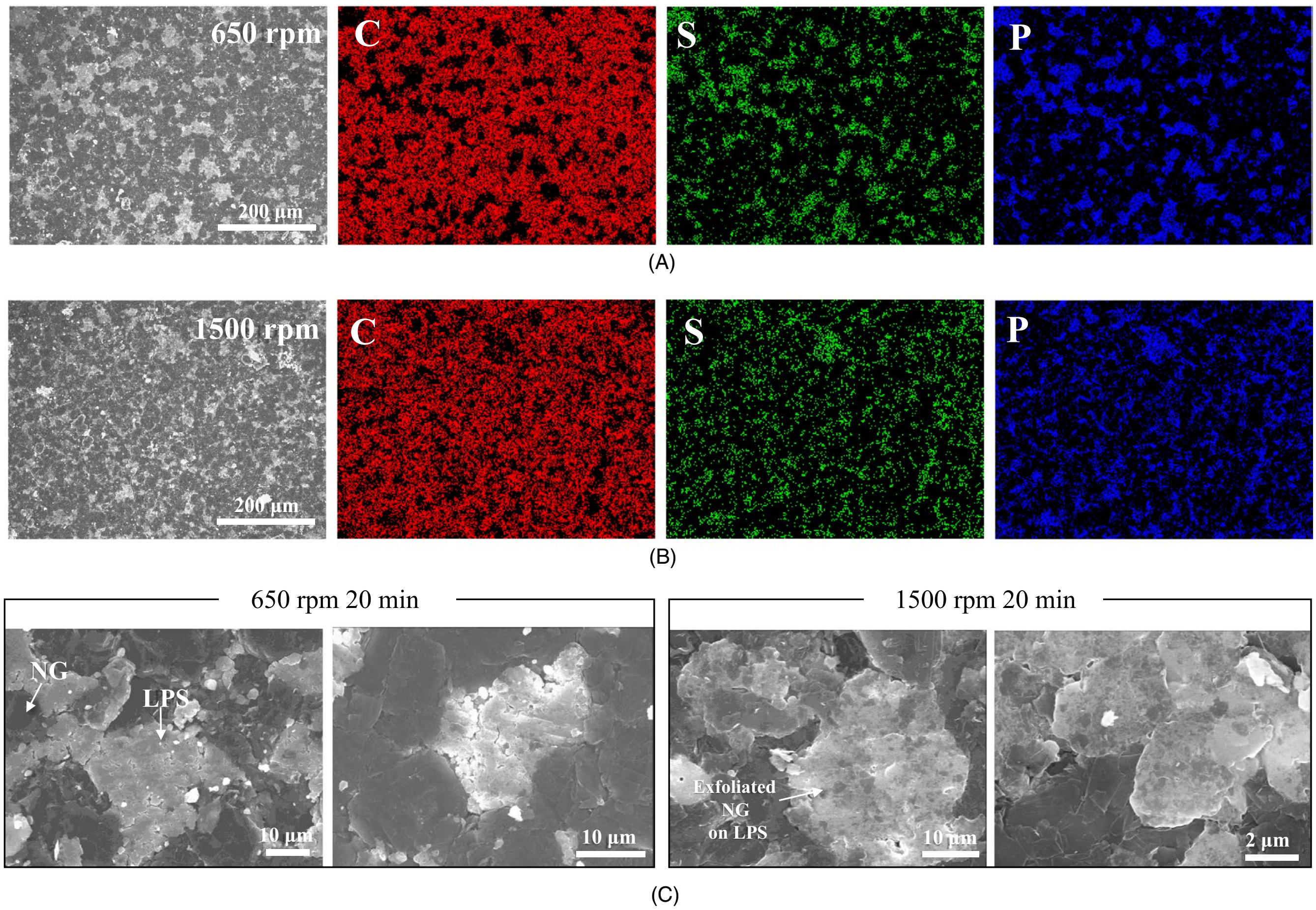

FIGURE 2 SEM and EDS images of composite electrodes mixed at (A) 650 rpm and (B) 1500 rpm and (C) higher resolution views of each electrode

the ion transport resistance within the composite electrodes (Figure 1C). The resistance of the composite electrodes mixed at 300, 650, and 1000 rpm was ~260 Ω, whereas that of the electrode mixed at 1500 rpm was ~1030 Ω, and a gradual increase in resistance was confirmed as the mixing speed increased above 1000 rpm.

To confirm the relationship between the ionic transport resistance and the cell performance, composite half-cells with a theoretical capacity of 3.38 mAh/cm^2 (loading level of 15.2 mg/cm^2) were fabricated and evaluated at rates of 0.1C and 0.3C for five cycles. The results showed that the three composite electrodes with similar resistances exhibited a similar discharge capacity of ~3 mAh/cm^2 at a charge/discharge rate of 0.1C, but the capacity of the composite mixed at 1500 rpm was ~2.56 mAh/cm^2, and the discharge capacity was significantly degraded. Furthermore, at an increased charge/discharge rate, the composite electrode mixed at 1500 rpm exhibited a capacity of ~1 mAh/cm^2, whereas the others had discharge capacities of over 2 mAh/cm^2. This significant capacity degradation is strongly related to the large resistance measured in Figure 1B and 1C. The large *IR* drop in the electrolyte may make it difficult to fully charge the active materials.

SEM analysis with EDS was performed to investigate the morphological changes in each composite electrode depending on the mixing conditions (Figure 2). We found no remarkable difference among the samples with similar capacities. However, the composite electrode mixed at 1500 rpm had a distinctively different morphology. The strong mixing process resulted in more uniform dispersion of NG and LPS particles in the composite electrode mixed at 1500 rpm than in the other samples (Figure 2A and 2B). The components of the composite electrode mixed at 650 rpm were dispersed to some degree, but localized NG and LPS regions also appeared. Therefore, simply considering the distributions of NG and LPS particles, the composite electrode mixed at a higher rotation speed seemed to be desirable for effective ionic conduction to the active material throughout the composite electrode. However, a high-resolution image revealed that many small particles decorated the surface of the LPS particles (Figure 2C), and we inferred that NG was exfoliated by ball milling at a high rotation speed, and fragments of NG became attached to the surfaces of the LPS particles (Figure S1) [23]. We speculated that eventually these fragments prevented facile ion transport among LPS particles by blocking the ionic pathway or increasing its tortuosity, which is highly

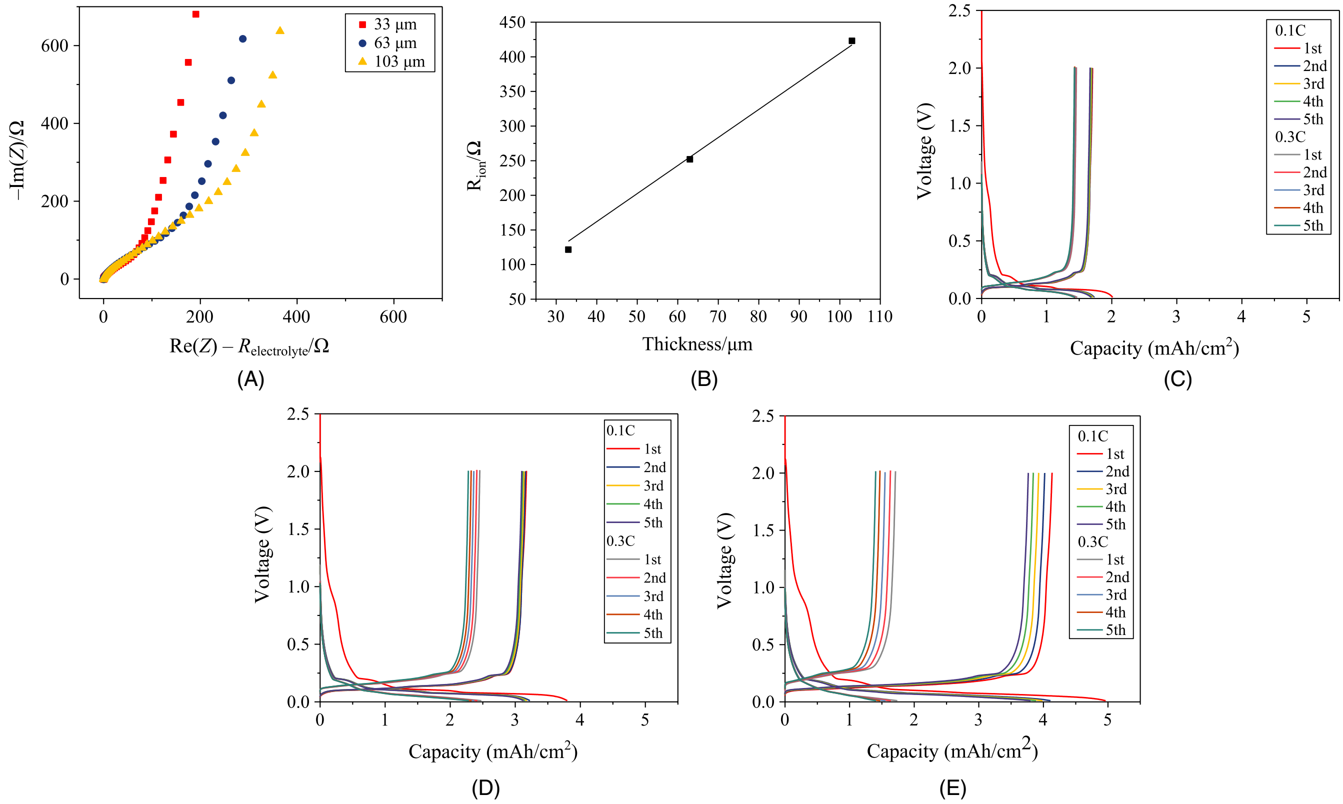

FIGURE 3 (A) Impedance results of composite electrodes of various thicknesses, (B) measured resistance versus composite thickness, and (C–E) charge/discharge profiles of composite electrodes

consistent with the high resistance measured in the symmetric cell (Figure 1B and 1C). In addition, this phenomenon may be related to the low Coulombic efficiency (62.28%) of the composite electrode mixed at 1500 rpm, which is attributed to the formation of a larger solid–electrolyte interphase owing to the increase in surface area due to exfoliation of NG (Figure 1G) [24]. Note that mild preparation of the composite electrode is essential [25,26].

All-solid-state batteries with high-energy-density generally require a thick composite electrode, but increasing the thickness of the electrode is likely to decrease the power performance owing to retardation of ion transport within thick electrodes [27]. To optimize the trade-off between the energy density and power density, we tested the performance of cells with different electrode thicknesses (~33, ~63, and ~103 μm) or areal capacities (1.69, 3.38, and 5.07 mAh/cm^2) (Figure 3). The impedance results of the symmetric cells confirmed that the composite electrode thickness is proportional to the ion transport resistance (Figure 3A and 3B). From a plot of these resistance values as a function of composite electrode thickness, we obtained the apparent ionic resistivity of the composite electrode with NG (60 wt%) and LPS (40 wt%) as ~5.35×10^2 Ωm (ionic conductivity: ~1.86×10^{-5} S/cm) (Figure 3B). The measured discharge capacities of the cells at 0.1C were ~1.68, ~3.13, and ~3.94 mAh/cm^2, which corresponded to 99.4%, 92.6%, and 77.8% of their theoretical capacities, respectively (Figure 3C). Notably, the increase in thickness clearly decreased the ratio of the measured capacities to the theoretical capacities, which suggested that increasing the resistance significantly impeded lithium-ion conduction to the active material, especially near the current collector (Figure 3B). This trend became more significant at a higher charge/discharge rate; the measured capacities and their ratios at 0.3C were ~1.44, ~2.35, and ~1.55 mAh/cm^2 and 85.2%, 69.7%, and 30.6%, respectively. Interestingly, the capacity of the cell with an electrode thickness of ~103 μm (~1.55 mAh/cm^2) was lower than that of the cell with an electrode thickness of ~63 μm (~2.35 mAh/cm^2) at 0.3C despite the large amount of active material, which indicates that good conduction within thick composite electrodes is particularly important for higher electrochemical performance [20].

To enhance the power density of all-solid-state batteries while maintaining high-energy-density, we demonstrate a precise composite design using a concentration gradient in the solid electrolyte (Figure 4). As the ionic conductance is proportional to the volume of the solid electrolyte, lithium ions can easily access all parts of the active material in the concentration-gradient composite electrode configuration, where the solid electrolyte concentration in the composite electrode increases toward the middle solid electrolyte layer (Figure 4A). The concentration-gradient composite electrode can be simply fabricated by sequential deposition of composite

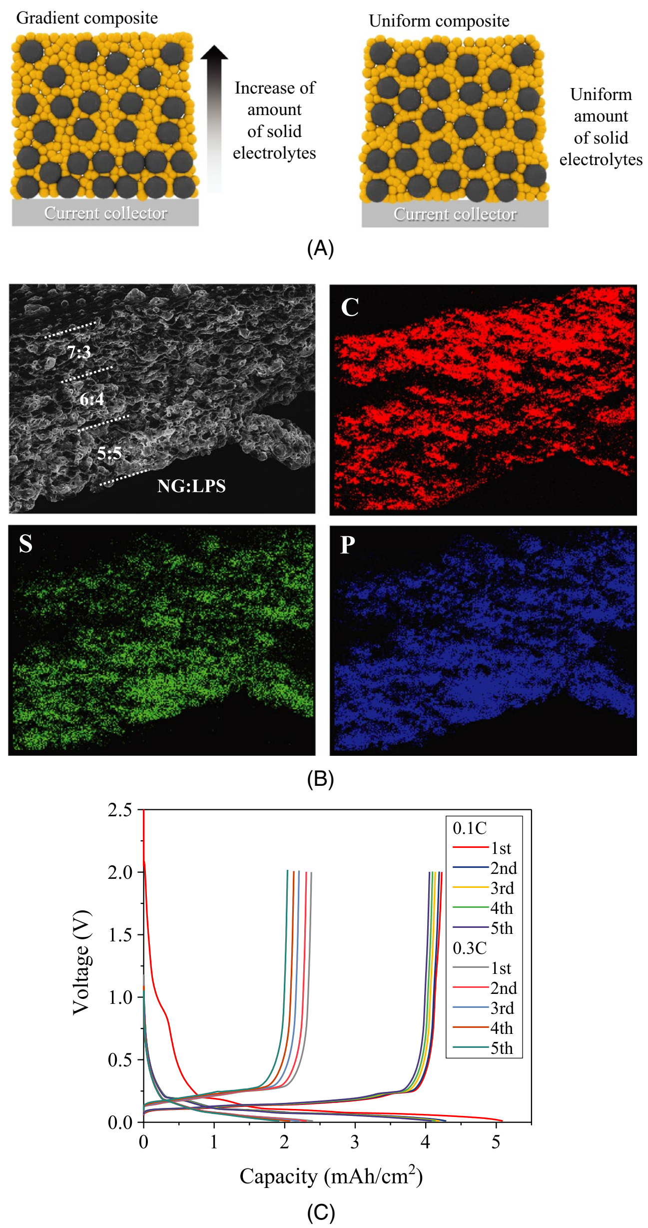

FIGURE 4 (A) Schematic illustrations of concentration-gradient and uniform composite electrodes and (B) SEM and EDS images and (C) charge/discharge profiles of the concentration-gradient electrode

powders with different ratios of NG and LPS. To confirm that a concentration gradient formed in the composite electrode, a tilted SEM observation with EDS was performed for a three-layered composite electrode (NG:LPS = 7:3, 6:4, and 5:5) and a uniform composite electrode. (For clear visualization, the thickness of the concentration-gradient composite electrode was increased.) As shown in Figure 4B, the upper region (NG:LPS = 7:3) had a higher C content than the lower region (NG:LPS = 5:5), and S and P exhibited the opposite trend. By contrast, C, S, and P were distributed uniformly in the uniform composite electrode (Figure S2). Note that the fabrication process can be further improved to form a continuous concentration gradient of a solid electrolyte and active materials.

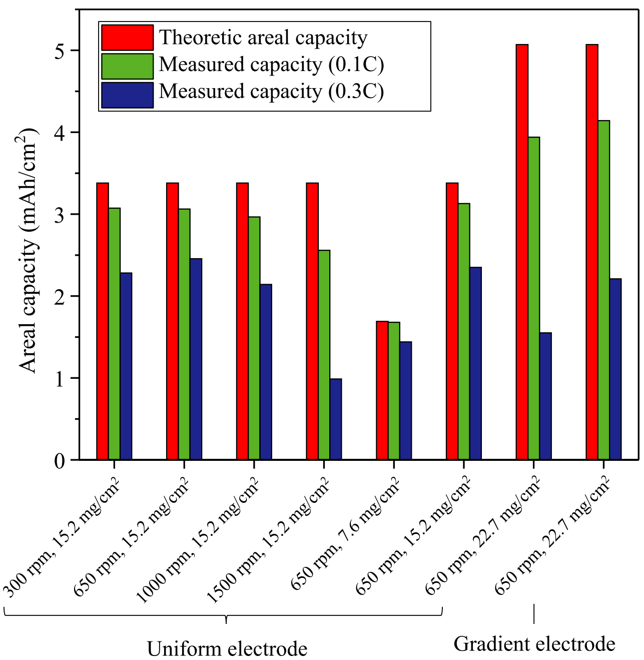

FIGURE 5 Capacities of the measured cells in this study

To obtain all-solid-state batteries with reasonable performance, we used concentration-gradient composite electrodes with a three-layered structure (NG:LPS = 7:3, 6:4, and 5:5) to fabricate a half-cell with a theoretical areal capacity of 5.07 mAh/cm^2. Before the half-cell test, we analyzed the impedance of the symmetric cells (Figure S3). This analysis revealed that the concentration-gradient composite electrode exhibited better impedance than the uniform composite electrode, but further detailed analysis must be conducted in future studies. The results of the half-cell test showed that the concentration-gradient electrode had a higher power density than the uniform composite electrode (Figures 3E and 4C). The capacities of the uniform and concentration-gradient electrodes at a charge/discharge rate of 0.1C were similar (~3.94 and ~4.142 mAh/cm^2, respectively), but at a charge/discharge rate of 0.3C, the capacity of the concentration-gradient composite was 2.21 mAh/cm^2, which was 42.6% higher than that of the uniform composite electrode. This result indicated that a simple change in the design of the composite electrodes can enhance the electrochemical performance even when identical components are used. Figure 5 summarizes the measured capacities of all the cells in this work for convenient comparison, and we again confirm that the concentration-gradient electrode can exhibit a reasonable energy density and power density. Further, to obtain a full cell with superior performance, it is necessary to optimize the middle solid electrolyte layer and composite cathodes, and we believe that a similar approach to tuning the composition of a solid electrolyte can be applied to composite cathodes as well.

4 | CONCLUSIONS

In summary, we presented a systematic study of composite electrodes consisting of an active material and a solid electrolyte in all-solid-state batteries. The ion transport properties were evaluated and compared using the TLM model of composite symmetric cells under various experimental conditions. It was confirmed that a strong mixing process can enhance the dispersity of the active material and solid electrolyte; however, fragmentation of active materials induced by severe ball milling can significantly impede ionic transport. Therefore, careful optimization is crucial to obtaining composite electrodes with desirable properties. Furthermore, to realize all-solid-state batteries with both high-energy-density and high-power-density, we investigated the cell performance using composite electrodes with various thicknesses and presented a concentration-gradient composite electrode. Our study confirmed that the electrochemical properties of the concentration-gradient composite electrode were better than those of a uniform composite electrode and provided a meaningful approach to enhancing cell performance by composite electrode design.

ORCID

Ju Young Kim https://orcid.org/0000-0002-2396-4457
Seok Hun Kang https://orcid.org/0000-0001-6725-7140
Kwang Man Kim https://orcid.org/0000-0002-4016-7265

REFERENCES

1. J. G. Kim et al., *A review of lithium and non-lithium based solid state batteries*, J. Power Sources **282** (2015), 299–322.
2. J. Lau et al., *Sulfide solid electrolytes for lithium battery applications*, Adv. Energy Mater. **8** (2018), 1800933:1–24.
3. J. Schnell et al., *All-solid-state lithium-ion and lithium metal batteries—paving the way to large-scale production*, J. Power Sources **382** (2018), 160–175.
4. S.-H. Kim et al., *Flexible/shape-versatile, bipolar all-solid-state lithium-ion batteries prepared by multistage printing*, Energy Environ. Sci. **11** (2018), 321–330.
5. B. Zhang et al., *Mechanisms and properties of ion-transport in inorganic solid electrolytes*, Energy Storage Mater. **10** (2018), 139–159.
6. K. H. Park et al., *Design strategies, practical considerations, and new solution processes of sulfide solid electrolytes for all-solid-state batteries*, Adv. Energy Mater. **8** (2018), 1800035:1–24.
7. A. Manthiram, X. Yu, and S. Wang, *Lithium battery chemistries enabled by solid-state electrolytes*, Nat. Rev. Mater. **2** (2017), 16103:1–17.
8. J. Y. Kim et al., *Reversible thixotropic gel electrolytes for safer and shape-versatile lithium-ion batteries*, J. Power Sources **401** (2018), 126–134.
9. D. O. Shin et al., *Synergistic multi-doping effects on the* $Li_7La_3Zr_2O_{12}$ *solid electrolyte for fast lithium ion conduction*, Sci. Rep. **5** (2015), 18053:1–9.
10. D. H. Kim et al., *Infiltration of solution-processable solid electrolytes into conventional Li-ion-battery electrodes for all-solid-state Li-ion batteries*, Nano Lett. **17** (2017), 3013–3020.
11. Y. Zhao and L. L. Daemen, *Superionic conductivity in lithium-rich anti-perovskites*, J. Am. Chem. Soc. **134** (2012), 15042–15047.
12. Y. Liu et al., *Development of the cold sintering process and its application in solid-state lithium batteries*, J. Power Sources **393** (2018), 193–203.
13. H. W. Kim et al., *Hybrid solid electrolyte with the combination of* $Li_7La_3Zr_2O_{12}$ *ceramic and ionic liquid for high voltage pseudo-solid-state Li-ion batteries*, J. Mater. Chem. A **4** (2016), 17025–17032.
14. K. Bi et al., *Improving low-temperature performance of spinel* $LiNi_{0.5}Mn_{1.5}O_4$ *electrode and* $LiNi_{0.5}Mn_{1.5}O_4/Li_4Ti_5O_{12}$ *full-cell by coating solid-state electrolyte Li-Al-Ti-P-O*, J. Power Sources **389** (2018), 240–248.
15. S. Yubuchi et al., *Preparation of high lithium-ion conducting* Li_6PS_5Cl *solid electrolyte from ethanol solution for all-solid-state lithium batteries*, J. Power Sources **293** (2015), 941–945.
16. K. H. Park et al., *Solution-processable glass* $LiI\text{-}Li_4SnS_4$ *superionic conductors for all-solid-state Li-ion batteries*, Adv. Mater. **28** (2016), 1874–1883.
17. A. Miura et al., *Liquid phase synthesis of sulfide electrolytes for all-solid-state lithium battery*, Nat. Rev. Chem. **3** (2019), 189–198.
18. A. Hayashi et al., *Formation of superionic crystals from mechanically milled* $Li_2S–P_2S_5$ *glasses*, Electrochem. Commun. **5** (2003), 111–114.
19. A. Sakuda, A. Hayashi, and M. Tatsumisago, *Sulfide solid electrolyte with favorable mechanical property for all-solid-state lithium battery*, Sci. Rep. **3** (2013), 2261.
20. N. Ogihara et al., *Impedance spectroscopy characterization of porous electrodes under different electrode thickness using a symmetric cell for high-performance lithium-ion batteries*, J. Phys. Chem. C **119** (2015), 4612–4619.
21. N. Kaiser et al., *Ion transport limitations in all-solid-state lithium battery electrodes containing a sulfide-based electrolyte*, J. Power Sources **396** (2018), 175–181.
22. R. de Levie, *On porous electrodes in electrolyte solutions—IV*, Electrochim. Acta **9** (1964), 1231–1245.
23. W. Zhao et al., *Preparation of graphene by exfoliation of graphite using wet ball milling*, J. Mater. Chem. **20** (2010), 5817–5819.
24. P. Guo, H. Song, and X. Chen, *Electrochemical performance of graphene nanosheets as anode material for lithium-ion batteries*, Electrochem. Commun. **11** (2009), 1320–1324.
25. J. Kim et al., *Effect of mixing method on the properties of composite cathodes for all-solid-state lithium batteries using Li2S–P2S5 solid electrolytes*, J. Power Sources **244** (2013), 476–481.
26. S. Noh et al., *Importance of mixing protocol for enhanced performance of composite cathodes in all-solid-state batteries using sulfide solid electrolyte*, J. Electroceram. **40** (2018), 293–299.
27. Y. Kato et al., *All-solid-state batteries with thick electrode configurations*, J. Phys. Chem. Lett. **9** (2018), 607–613.

AUTHOR BIOGRAPHIES

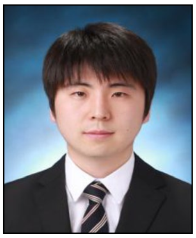

Ju Young Kim received his BS, MS, and PhD degrees in materials science and engineering from Korea Advanced Institute of Science and Technology (KAIST), Daejeon, Rep. of Korea, in 2009, 2011, and 2015, respectively. Since 2016, he has been working for the ETRI, Daejeon, Rep. of Korea. His main research interests are nanofabrication and energy storage devices, including lithium metal secondary batteries and all-solid-state batteries.

Jumi Kim received her BS degree in electrical engineering from Hanbat National University in Daejeon, Rep. of Korea, in 2008 and her MS degree in an interdisciplinary course on photovoltaic system engineering from Sungkyunkwan University in Suwon, Rep. of Korea, in 2010. Since 2010, she has been working for the ETRI, Daejeon, Rep. of Korea. Her research covers various materials and fabrication of energy storage devices, including lithium-ion secondary batteries, and solid-state batteries.

Seok Hun Kang received his BS degree in materials science and engineering from Korea Advanced Institute of Science and Technology (KAIST), Daejeon, Rep. of Korea, in 2014, and his MS degree in materials science and engineering from KAIST in 2016. Since 2016, he has been working for the ETRI, Daejeon, Rep. of Korea. His main research interests are carbon-based nanomaterials and energy storage devices.

Dong Ok Shin received his BS degree in materials science and engineering from Hanyang University, Rep. of Korea, in 2006 and his MS and PhD degrees in materials science and engineering from Korea Advanced Institute of Science and Technology (KAIST), Daejeon, Rep. of Korea, in 2008 and 2012, respectively. Since 2012, he has been working for the ETRI, Daejeon, Rep. of Korea. His main research interests are nanopatterning, nanofabrication, and energy storage devices, including lithium metal secondary batteries, all-solid-state batteries, and sodium ion secondary batteries.

Myeong Ju Lee received her BS degree in advanced materials engineering from Daejeon University, Daejeon, Rep. of Korea, in 2014. She began an MS/PhD integration course at the University of Science and Technology (UST) and joined ETRI as a student researcher in 2016. Her main research interest is energy storage devices, including lithium metal secondary batteries, and all-solid-state batteries.

Jimin Oh received his BS degree in electrical and electronic engineering and his MS degree in electrical engineering from Kyoto University, Japan, in 2008 and 2010, respectively. He has been working toward the PhD degree in materials science and engineering from Korea Advanced Institute of Science and Technology (KAIST), Daejeon, Rep. of Korea since 2018. He is also currently a Senior Researcher with the Electronics and Telecommunications Research Institute (ETRI), Daejeon, South Korea. His main research interests include multi-scale analysis and fabrication optimization of energy storage devices, including high-energy-density lithium-ion batteries and all-solid-state batteries, and energy conversion/control systems, including brushless direct current (BLDC) motor driver IC design, DC/DC converters, and battery management systems.

Young-Gi Lee received his BS degree in chemical engineering from Pusan National University, Rep. of Korea, in 1995 and his MS and PhD degrees in chemical engineering and polymer materials from the Korea Advanced Institute of Science and Technology in Daejeon, Rep. of Korea, in 1997 and 2001, respectively. He joined the ETRI in 2001, where he has been working for the Reality Devices Research Division. His current research topics are the establishment of various solid electrolyte systems for lithium rechargeable batteries and wearable, flexible primary and secondary batteries and their fabrication.

Kwang Man Kim received his BS degree in chemical engineering from Yonsei University, Seoul, Rep. of Korea, in 1985 and his MS and PhD degrees in chemical engineering from the Korea Advanced Institute of Science and Technology, Seoul and Daejeon, Rep. of Korea, in 1988 and 1995, respectively. He was with the Research Institute of Industrial Science & Technology (RIST), Pohang, Rep. of Korea, from 1988 to 1991 and the Hyosung R&D Center, Gumi, Rep. of Korea, from 1997 to 1998. He joined the ETRI in 1999 and has been working with the ICT Creativity Research Lab., where he has studied various materials and fabrication processes for versatile (for example, wearable, flexible, and solid-state) power source devices, including supercapacitors and lithium rechargeable batteries. He has published over 140 papers in SCI journals and has over 60 international and domestic patents.

SUPPORTING INFORMATION

Additional supporting information may be found online in the Supporting Information section at the end of the article.